Article

Enhanced Cementation of Co^{2+} and Ni^{2+} from Sulfate and Chloride Solutions Using Aluminum as an Electron Donor and Conductive Particles as an Electron Pathway

Sanghyeon Choi [1,*,†] , Sanghee Jeon [2,†], Ilhwan Park [2], Mayumi Ito [2] and Naoki Hiroyoshi [2]

[1] Division of Sustainable Resources Engineering, Graduate School of Engineering, Hokkaido University, Sapporo 060-8628, Japan
[2] Division of Sustainable Resources Engineering, Faculty of Engineering, Hokkaido University, Sapporo 060-8628, Japan; shjun1121@eng.hokudai.ac.jp (S.J.); i-park@eng.hokudai.ac.jp (I.P.); itomayu@eng.hokudai.ac.jp (M.I.); hiroyosi@eng.hokudai.ac.jp (N.H.)
* Correspondence: cshshow351@gmail.com; Tel.: +81-11-706-6315
† These authors have contributed equally to this work and share first authorship.

Abstract: Cobalt and nickel have become important strategic resources because they are widely used for renewable energy technologies and rechargeable battery production. Cementation, an electrochemical deposition of noble metal ions using a less noble metal as an electron donor, is an important option to recover Co and Ni from dilute aqueous solutions of these metal ions. In this study, cementation experiments for recovering Co^{2+} and Ni^{2+} from sulfate and chloride solutions (pH = 4) were conducted at 298 K using Al powder as electron donor, and the effects of additives such as activated carbon (AC), TiO_2, and SiO_2 powders on the cementation efficiency were investigated. Without additives, cementation efficiencies of Co^{2+} and Ni^{2+} were almost zero in both sulfate and chloride solutions, mainly because of the presence of an aluminum oxide layer (Al_2O_3) on an Al surface, which inhibits electron transfer from Al to the metal ions. Addition of nonconductor (SiO_2) did not affect the cementation efficiencies of Co^{2+} and Ni^{2+} using Al as electron donor, while addition of (semi)conductors such as AC or TiO_2 enhanced the cementation efficiencies significantly. The results of surface analysis (Auger electron spectroscopy) for the cementation products when using TiO_2/Al mixture showed that Co and Ni were deposited on TiO_2 particles attached on the Al surface. This result suggests that conductors such as TiO_2 act as an electron pathway from Al to Co^{2+} and Ni^{2+}, even when an Al oxide layer covered on an Al surface.

Keywords: cementation; cobalt (Co); nickel (Ni); aluminum (Al); titanium dioxide (TiO_2); silicon dioxide (SiO_2)

1. Introduction

Cementation, an electrochemical deposition of noble metal ions by a less noble metal as an electron donor, is usually applied to remove/recover metal ions from dilute aqueous solutions [1–4]. The advantages of cementation are (1) recovery of metals in zero-valent form, (2) simple methods, and (3) low-energy consumption [2,5]. In this method, the overall reaction of cementation is given by Equation (1) [6–8]:

$$mN^0 + nM^{m+} \rightarrow mN^{n+} + nM^0 \tag{1}$$
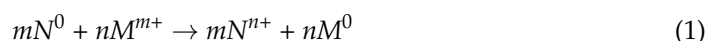
The cementation reaction is divided into anodic (Equation (2)) and cathodic reactions (Equation (3)):

$$\text{Anodic } mN^0 \rightarrow mN^{n+} + nme^- \tag{2}$$

$$\text{Cathodic } nM^{m+} + nme^- \rightarrow nM^0 \tag{3}$$
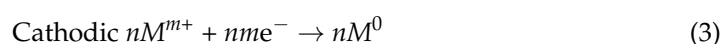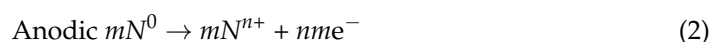
The noble metal ions (M^{m+}) are deposited on the surface of a less noble elemental metal (N^0) spontaneously, and the driving force of this reaction is mainly determined by differences in the standard electrode potentials for M^{n+}/M^0 and N^{n+}/N^0 redox pairs, and it increases when the electrode potential of N^0 is low.

Aluminum (Al) can be considered as a strong reductant (electron donor) used for cementation because of its extremely low standard electrode potential (i.e., $E^0_{Al3+/Al} = -1.67$ V vs. standard hydrogen electrode (SHE)) [7,9–11]. The practical application of Al for cementation, however, is limited due to the presence of a dense Al oxide layer (Al_2O_3) on the Al surface, which inhibits electron transfer from Al^0 to metal ions [9,12,13]. When the Al oxide layer is removed from the surface, Al can be used as an electron donor for cementation. To remove the Al oxide layer, however, high temperatures, acid/alkaline solutions, or high concentration of chloride ions are needed [2,5,9,14,15], and these extreme conditions make it difficult to use Al as an electron donor in the practical cementation processes.

Recently, the authors investigated the effects of activated carbon (AC) addition on the efficiency of cementation using Al as an electron donor for recovering gold ions from ammonium thiosulfate solution [16,17], and heavy metal ions (Co^{2+}, Ni^{2+}, Zn^{2+}, and Cd^{2+}) from acidic sulfate and chloride solutions. The results showed that cementation efficiencies of the metal ions were significantly enhanced by the addition of activated carbon (AC) even when an insulating Al oxide layer covered on the Al surface [16,17]. This "enhanced cementation using AC/Al-mixture" can be operated under mild conditions; i.e., it does not require extreme operating conditions such as high temperatures, and high concentrations of chemical reagent such as acid, base, and chloride ions. This new method may, therefore, provide a practical way to use Al, one of the strongest reductants (electron donor) for cementation to recover metal ions from dilute solutions.

Although the details of the mechanism of enhanced cementation using the AC/Al-mixture are not yet fully understood, the results of surface analysis for the cementation products have suggested that AC attached on the Al surface acted as an electron pathway from Al to noble metal ions, even in the presence of a surface Al oxide layer [17]. If this is the case and the essential role of AC is just as an electron pathway, enhanced cementation would occur even when AC is replaced by other (semi)conductors. On the other hand, as AC is a porous material and has a very large specific surface area [18], not only the electroconductivity but also large adsorption capacity of AC for metal ions may play an important role in the enhanced cementation using the AC/Al-mixture. If this is the case, replacing AC to another conductor with a low specific surface area cannot enhance the cementation using Al as an electron donor.

Cobalt (Co) and nickel (Ni) represent important strategic resources in the world market and their use is rapidly growing for renewable energy technologies and rechargeable battery productions, and the importance of the development of technologies for recovering and purifying Co and Ni is continuously increasing [19–24]. Therefore, this study aims to investigate whether the AC could be replaced with other (semi)conductors for recovery of Co and Ni from sulfate and chloride solutions. Titanium dioxide (TiO_2) was selected for a semiconductor because of its nontoxic, nonreactive, and high chemical stability, while silicon dioxide (SiO_2) was chosen for a nonconductor to clarify the mechanism(s) of the enhanced cementation using the mixture of conductor and Al [25,26].

In the present study, batch-type cementation experiments were conducted using Al as an electron donor to recover Co^{2+} and Ni^{2+} from sulfate and chloride solutions and the effects of the addition of AC, TiO_2, or SiO_2 on the recoveries of these metal ions were investigated. Surface analysis (Auger electron spectroscopy (AES)) for the cementation products were also conducted to elucidate the cementation mechanism.

2. Materials and Methods

2.1. Materials

As an electron donor, Al powder (99.99%, Wako Pure Chemical Industries, Ltd., Osaka, Japan) was used, and AC powder (99.99%, Wako Pure Chemical Industries, Ltd., Osaka,

Japan), TiO₂ powder (99.0%, rutile form, Wako Pure Chemical Industries, Ltd., Osaka, Japan), and SiO₂ powder (99.0%, Wako pure Chemical Industries, Ltd., Osaka, Japan) were used as additives. Particle size distribution of these materials, measured by laser diffraction (Microtrac® MT3300SX, Nikkiso Co. Ltd., Osaka, Japan), is shown in Figure 1. The median diameters (D_{50}) of Al, AC, TiO₂, and SiO₂ were 21.3, 38.1, 8.5, and 21.2 μm, respectively.
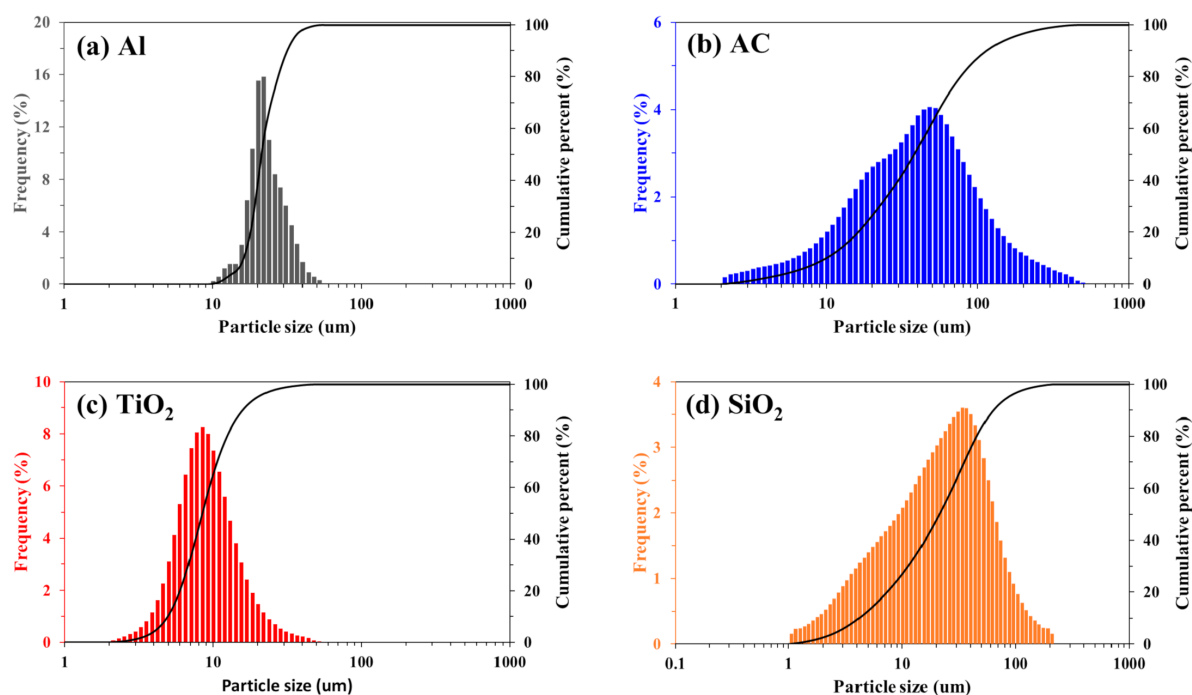

Figure 1. Particle size distribution for (**a**) aluminum (Al), (**b**) activated carbon (AC), (**c**) titanium dioxide (TiO₂), and (**d**) silicon dioxide (SiO₂) used in this study.

2.2. Recovery of Co^{2+} and Ni^{2+} from Sulfate and Chloride Solutions

2.2.1. Preparation of Co^{2+} and Ni^{2+} Solutions

The sulfate solutions containing 1 mM metal ions were prepared by dissolving CoSO₄·7H₂O (99.0%, Wako Pure Chemical Industries, Ltd., Osaka, Japan) or NiSO₄·6H₂O (99.0%, Wako Pure Chemical Industries, Ltd., Osaka, Japan) in deionized (DI) water (18 MΩ·cm, Mill-Q® Integral Water Purification System, Merck Millipore, Burlington, Vermont, USA). For the preparation of 1 mM metal chloride solutions, CoCl₂·6H₂O (99.0%, Kishida Chemical Co., Ltd., Osaka, Japan), or NiCl₂·6H₂O (98.0%, Kishida Chemical Co., Ltd., Osaka, Japan) was dissolved in DI water. The initial pH of sulfate and chloride solutions was adjusted to 4.0 using 1 M H₂SO₄ and HCl (Wako Pure Chemical Industries, Ltd., Osaka, Japan), respectively. The total concentration of SO₄²⁻ and Cl⁻ were fixed to 0.1 M using Na₂SO₄ (99.0%, Wako Pure Chemical Industries, Ltd., Osaka, Japan) and NaCl (99.5%, Wako Pure Chemical Industries, Ltd., Osaka, Japan) to normalize their effects on experiments.

2.2.2. Cementation Tests

The cementation tests were carried out in a 50 mL Erlenmeyer flask using a thermostat water bath shaker (Cool bath shaker, ML-10F, Taitec Corporation, Saitama, Japan) with 40 mm of shaking amplitude and 120 min⁻¹ of shaking frequency at 25 °C for 24 h. (Note that these parameters were selected based on our preliminary experiments). Ten milliliters of the prepared solution were added to the flask, then ultrapure nitrogen gas (99.9%) was introduced for 15 min before experiments to maintain an oxygen-free environment. One-tenth gram of Al powder and/or a predetermined amount (0.01, 0.05, 0.1, 0.2, 0.4 g)

of additive (i.e., AC, TiO$_2$, and SiO$_2$) were added to the solution. Ultrapure nitrogen gas (99.9%) was further introduced to the flask for 5 min, then the flask was tightly capped with a rubber cap and sealed with parafilm, and an experiment was conducted. After 24 h, the suspension was filtered using a syringe-driven membrane filter (pore size: 0.2 μm, LMS Co., Ltd., Tokyo, Japan); final pH of the filtrate was measured. The filtrate was diluted with 0.1 M HNO$_3$, and the concentrations of metal ions were analyzed by inductively coupled plasma atomic emission spectroscopy (ICP-AES, ICPE-9820, Shimadzu Corporation, Kyoto, Japan). The recovery efficiency of Co^{2+} and Ni^{2+} was calculated based on Equation (4):

$$\text{Recovery efficiency, } R = \frac{C_i - C_f}{C_i} \tag{4}$$

where C_i and C_f are the initial and final concentrations of metal ions, respectively.

2.2.3. Surface Analysis

The solid products obtained by filtration were washed 5 times with DI water, dried in a vacuum oven at 40 °C for 24 h, and then analyzed by Auger electron spectroscopy (AES) using JAMP-9500F (JEOL Co., Ltd., Tokyo, Japan). The dried residue was mounted on an AES holder using conductive carbon tape. The analysis was conducted under the following conditions: ultrahigh vacuum condition, ~1 × 10^{-7} Pa; probe energy, 10 kV; and probe current, 19.7 nA. The spectra were analyzed by using Spectra Investigator AES software.

3. Results and Discussion

3.1. Recovery of Co^{2+} and Ni^{2+}

3.1.1. Recovery of Co^{2+} and Ni^{2+} from Sulfate Solution

Cementation experiments for recovering Co^{2+} and Ni^{2+} from sulfate solutions (initial pH = 4) were conducted for 24 h using Al powder as an electron donor, and the effects of the dosage of additives (AC, TiO$_2$, and SiO$_2$) on the efficiency of Co and Ni recoveries were investigated. To access the adsorption of Co^{2+} and Ni^{2+} on the additives, experiments without Al were also conducted.

Figures 2a–c and 3a–c show the Co and Ni recovery efficiencies and final pH as a function of SiO$_2$, AC, and TiO$_2$ dosages, respectively. In all experiments, final pH was in the range from 5.1 to 5.6, at which Co^{2+} and Ni^{2+} do not precipitate as their hydroxide (Figures S1 and S2).

As shown in Figures 2a and 3a, without Al, the efficiencies of Co and Ni recovery were almost 0% at any dosage of SiO$_2$, suggesting that there was no adsorption of Co^{2+} and Ni^{2+} on the SiO$_2$ surface. Even with Al, the Co and Ni recovery efficiencies were also almost 0% regardless of SiO$_2$ dosage, suggesting that cementation of Co^{2+} and Ni^{2+} using Al as an electron donor did not occur. This may be due to the presence of an Al oxide layer covering the Al surface, which inhibits the electron transportation from Al to Co^{2+} and Ni^{2+} [2,27]. Because the cementation did not occur regardless of SiO$_2$ addition, the results also confirm that physical breakage of the Al oxide layer due to the collision of SiO$_2$ to Al powder in the shaking flask did not cause enhanced cementation.

As shown in Figures 2b and 3b, even without Al, the recovery efficiency of Co^{2+} and Ni^{2+} increased with increasing AC dosage, suggesting that these metal ions adsorbed on the AC surface. It has been reported that there are functional groups such as carboxyl and carbonyl groups on the surface of the activated carbon and they act as adsorption sites to metal ions through the reaction described by Equation (5) [18,28,29]. Increase in final pH indicates that not only Co^{2+} and Ni^{2+}, but also proton (H$^+$) adsorbed on AC [30,31].

$$\text{-C-COOH} + \text{M}^{2+} \rightarrow \text{-C-COOM} + 2\text{H}^+ \text{ (M = Co or Ni)} \tag{5}$$
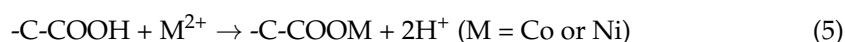
In the range between 0.05 to 0.2 g AC dosage, recovery efficiency was much higher with Al than without Al; at 0.1 g AC dosage, the efficiency was 56% for Co and 61% for Ni with Al, while it was 31% for Co and 43% for Ni without Al. The difference of metal

recovery efficiency between either with or without Al was 25% for Co and 18% for Ni, which cannot be ignored as an experimental error. This suggests that the addition of AC enhances Co and Ni cementation using Al as an electron donor (Equations (6) and (7)), even though the Al oxide layer remained on the Al surface.

$$3Co^{2+} + 2Al^0 \rightarrow 3Co^0 + 2Al^{3+} \tag{6}$$

$$3Ni^{2+} + 2Al^0 \rightarrow 3Ni^0 + 2Al^{3+} \tag{7}$$
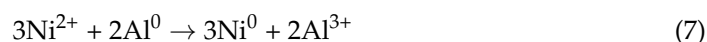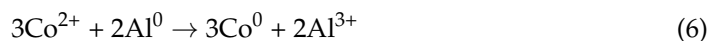
Following these equations, it is expected that the stoichiometric amount of Al dissolves when cementation occurs; however, the dissolved Al concentration after cementation was less than 3 ppm (Tables S1 and S2), which means that most of the Al^{3+} was precipitated as Al-(oxy)hydroxide [7,32].
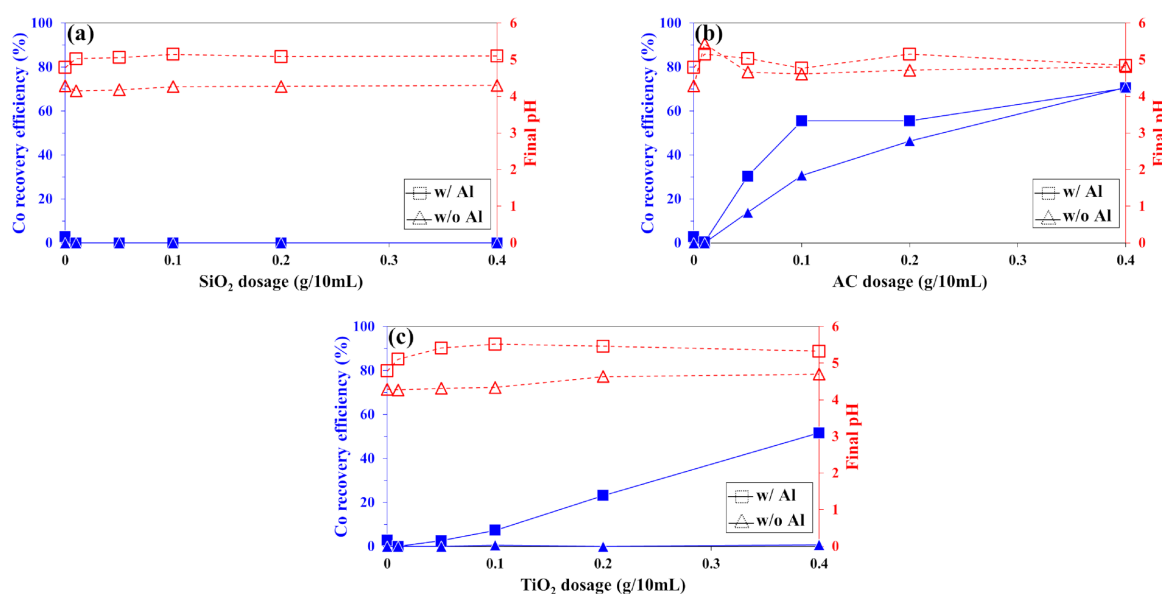

Figure 2. The effects of (**a**) SiO_2, (**b**) AC, and (**c**) TiO_2 dosages on the recovery efficiency of Co^{2+} and final pH in sulfate solutions at initial pH 4.0 for 24 h.
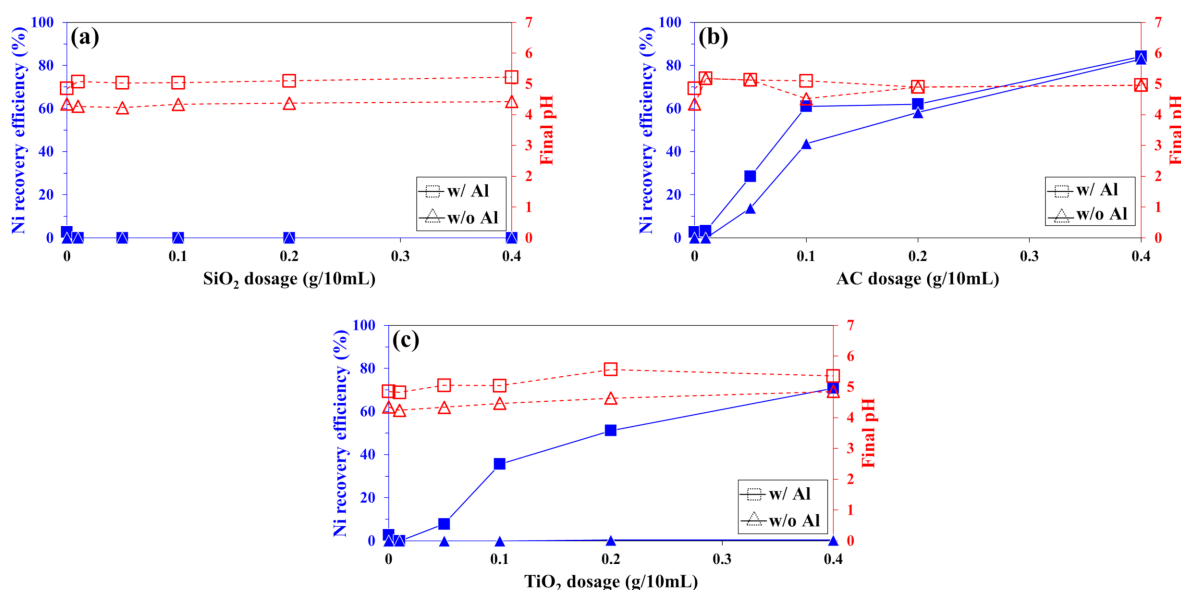

Figure 3. The effects of (**a**) SiO_2, (**b**) AC, and (**c**) TiO_2 dosages on the recovery efficiency of Ni^{2+} and final pH in sulfate solutions at initial pH 4.0 for 24 h.

As shown in Figures 2c and 3c, the recovery efficiency of Co^{2+} and Ni^{2+} without Al was almost 0% regardless of TiO_2 dosage, indicating that TiO_2 has no ability to adsorb Co^{2+} and Ni^{2+}. When 0.1 g of Al was used together with TiO_2, the recovery efficiency continuously increased with increasing TiO_2 dosage and reached the maximum value of 52% for Co and 71% for Ni with 0.4 g TiO_2. As already discussed, Co^{2+} and Ni^{2+} do not precipitate as hydroxides at the pH ranges observed in this series of experiments; the enhanced recovery of Co^{2+} and Ni^{2+} with TiO_2 and Al suggests that the addition of TiO_2 enhanced the cementation of Co^{2+} and Ni^{2+} by Al (Equations (6) and (7)). It was also confirmed that the dissolved Ti concentrations were below detection limit, indicating that TiO_2 is stable enough to be used as an agent to enhance cementation of Co^{2+} and Ni^{2+} with Al in the sulfate solution (Tables S1 and S2).

3.1.2. Recovery of Co^{2+} and Ni^{2+} from Chloride Solution

Cementation experiments for recovering Co^{2+} and Ni^{2+} from chloride solutions (initial pH = 4) were conducted for 24 h using Al powder as an electron donor, and the effects of the dosage of additives (AC, TiO_2, and SiO_2) on the efficiency of Co and Ni recovery were investigated. To access the adsorption of Co^{2+} and Ni^{2+} on the additives, experiments without Al were also conducted. Figures 4a–c and 5a–c show the Co and Ni recovery efficiencies and final pH as a function of AC, TiO_2, and SiO_2 dosages, respectively.

Similar to the sulfate system (Figures 2 and 3), final pH values of the chloride solutions (Figures 4 and 5) were less than 5.5 for Co and 6.1 for Ni (Tables S3 and S4), which means that removal of Co^{2+} and Ni^{2+} from the solutions by the formation of cobalt and nickel hydroxide precipitation does not need to be considered in this series of experiments (Figures S3 and S4).

It has been reported that in the presence of high concentrations of Cl^-, the Al oxide layer was dissolved and removed from the Al surface [13,33–35]. If the Al oxide layer is dissolved, a high concentration of dissolved Al would be detected in the solutions, but the observed results (Tables S3 and S4) showed that concentrations of Al were less than 5 ppm under all conditions. This implies that removal of the Al oxide layer did not occur under the experimental condition used here.

As shown in Figures 4a and 5a, when SiO_2 was used as an additive, the recovery efficiencies of Co^{2+} and Ni^{2+} both with and without Al were almost 0%. This indicates that in chloride solutions, Co^{2+} and Ni^{2+} were not adsorbed on SiO_2, and the cementation of Co and Ni with Al did not occur.

The results shown in Figures 4b and 5b suggest that adsorption of Co^{2+} and Ni^{2+} on AC occurred in chloride solutions, because in the absence of Al, recovery efficiencies of these ions increased with increasing AC dosage. As in sulfate solutions, in the presence of AC, enhancement of metal ion recovery by Al addition was confirmed (Figures 4b and 5b); e.g., at 0.1 g AC dosage, by adding Al, the efficiency increased from 57% to 70% for Co, and it increased from 57% to 70% for Ni. This suggests that enhanced cementation of these metal ions with AC occurred in chloride solutions.

Figures 4c and 5c show that the efficiencies of Co^{2+} and Ni^{2+} recovery in the absence of Al were almost 0% at any dosage of TiO_2, suggesting that adsorption of these ions on TiO_2 can be ignored. In the presence of Al, the efficiencies of Co^{2+} and Ni^{2+} recovery increased with increasing TiO_2 dosage; without TiO_2, the efficiencies were almost 0% for both Co and Ni while they increased to 61% for Co^{2+} and 99.9% for Ni^{2+} when 0.4 g TiO_2 was added. These results suggest clearly that addition of TiO_2 enhanced the cementation of Co and Ni by using Al as an electron donor, and indicated that AC can be replaced with TiO_2 even if its surface area is lower than AC [18,36,37].
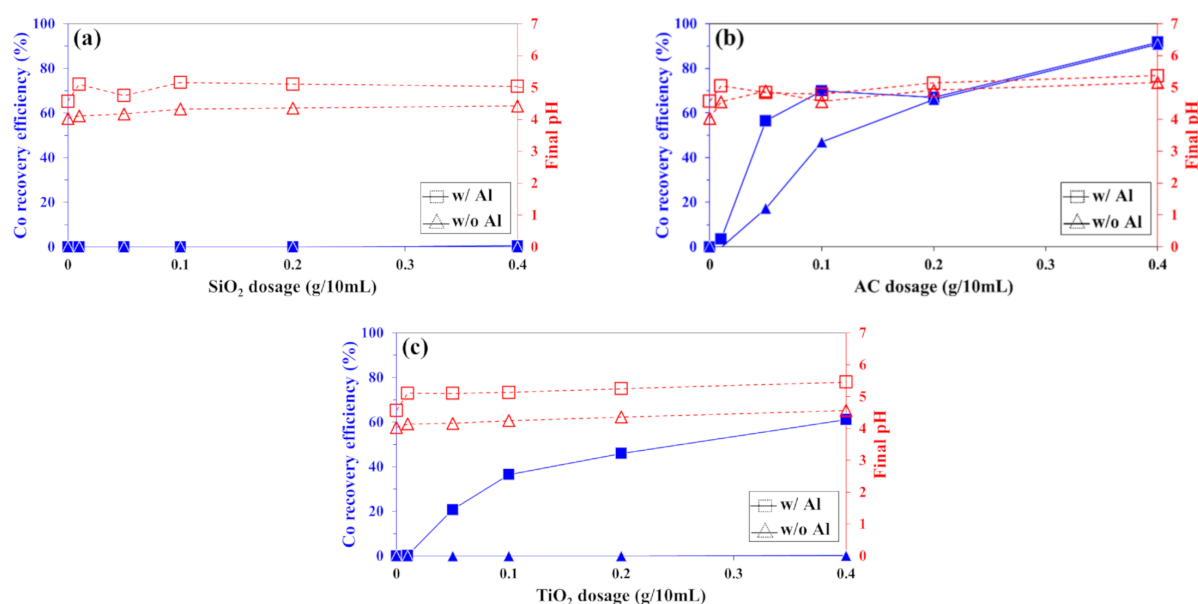
Figure 4. The effects of (**a**) SiO_2, (**b**) AC, and (**c**) TiO_2 dosages on the recovery efficiency of Co^{2+} and final pH in chloride solutions at initial pH 4.0 for 24 h.
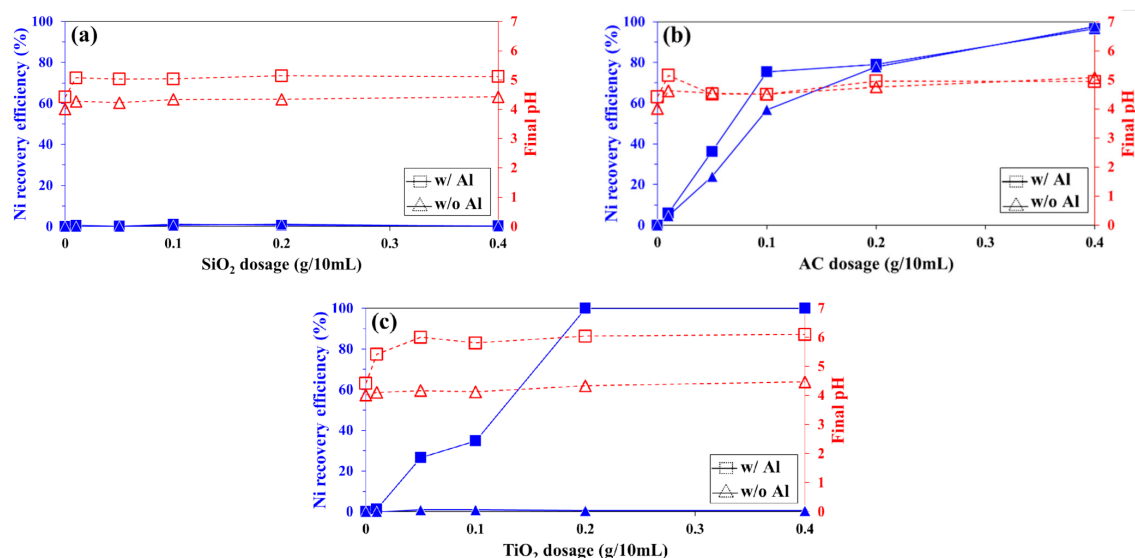

Figure 5. The effects of (**a**) SiO_2, (**b**) AC, and (**c**) TiO_2 dosages on the recovery efficiency of Ni^{2+} and final pH in chloride solutions at initial pH 4.0 for 24 h.

3.2. Surface Analysis of Deposited Co and Ni

To investigate the elemental compositions of the deposited Co and Ni, residues obtained from the Co^{2+} and Ni^{2+} recovery experiment from chloride solutions using 0.4 g of TiO_2 and 0.1 g of Al were analyzed by AES. Figures 6 and 7 show the AES photomicrographs (Figures 6a and 7a) and scan results of Co (Figure 6b,c) and Ni (Figure 7b,c). In both AES photomicrographs, many small gray particles and light particles are attached together onto the surface of the dark particle. The wide AES spectra of the dark particle (point 1 in Figures 6b and 7b) show strong signals of Al and O, indicating that these particles are assigned to Al powder. The small gray particles correspond to TiO_2 because of Ti and O signals observed at point 2 in Figures 6b and 7b. Meanwhile, light particles are observed at point 3 in Figures 6b and 7b are most likely the deposited Co and Ni, respectively.

To identify the elemental composition of the deposited Co and Ni, the narrow AES spectra in the range of 750–785 eV for Co and 830–858 eV for Ni were analyzed (Figures 6c and 7c). These spectra were fitted using reference spectra of Co, CoO, and Co_3O_4 for Co composition, and Ni and NiO for Ni composition. Fitting results indicate that the deposited Co consisted of metallic Co (93.1%) and CoO (6.9%), while the deposited Ni was composed of metallic Ni (86.2%) and NiO (13.8%). The analysis range of Auger is 0.3–5 nm, which is a near-surface analysis [38], so it is speculated that only the outermost surfaces of deposited Co and Ni were oxidized due to the oxidation of metallic Co and Ni during the dry process.

These results suggest that Co and Ni were deposited on TiO_2 particles attached to the Al surface and TiO_2 can act as an electron pathway from Al to Co^{2+} and Ni^{2+}, even if the Al oxide layer remains on the Al surface. These results showed that physical separation (i.e., ultrasonification) could be applied as the postcementation process for Co/Ni–TiO_2 particle and Al separation. Afterward, it is expected that only Co and Ni would be dissolved in aqueous solutions, while TiO_2 would not be dissolved because TiO_2 is more stable than Co and Ni.
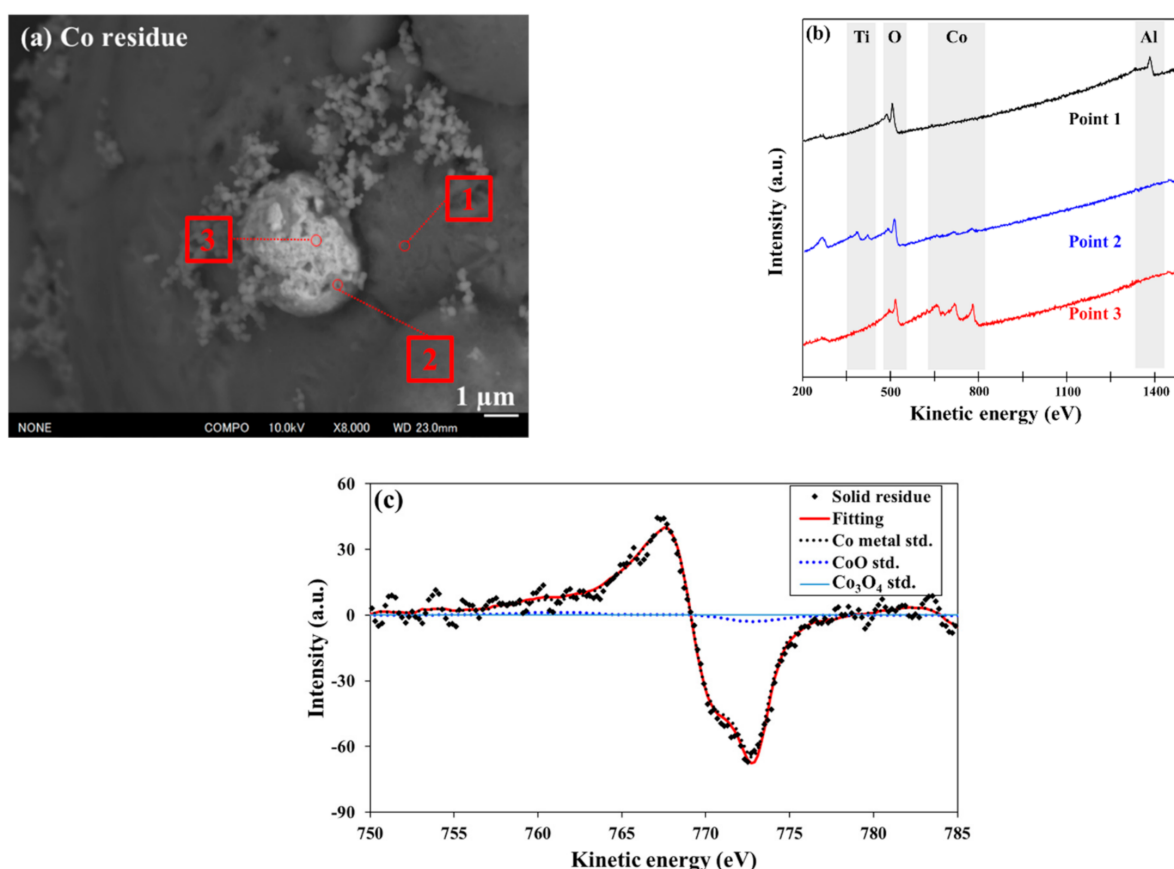

Figure 6. Auger electron spectroscopy (AES) results of the residue obtained after cementation of Co^{2+} from chloride solution using TiO_2/Al: (**a**) photomicrograph, (**b**) wide scan energy spectrum of each point, and (**c**) the narrow scan energy spectrum of the Co peak with fitting spectra of Co, CoO, and Co_3O_4.
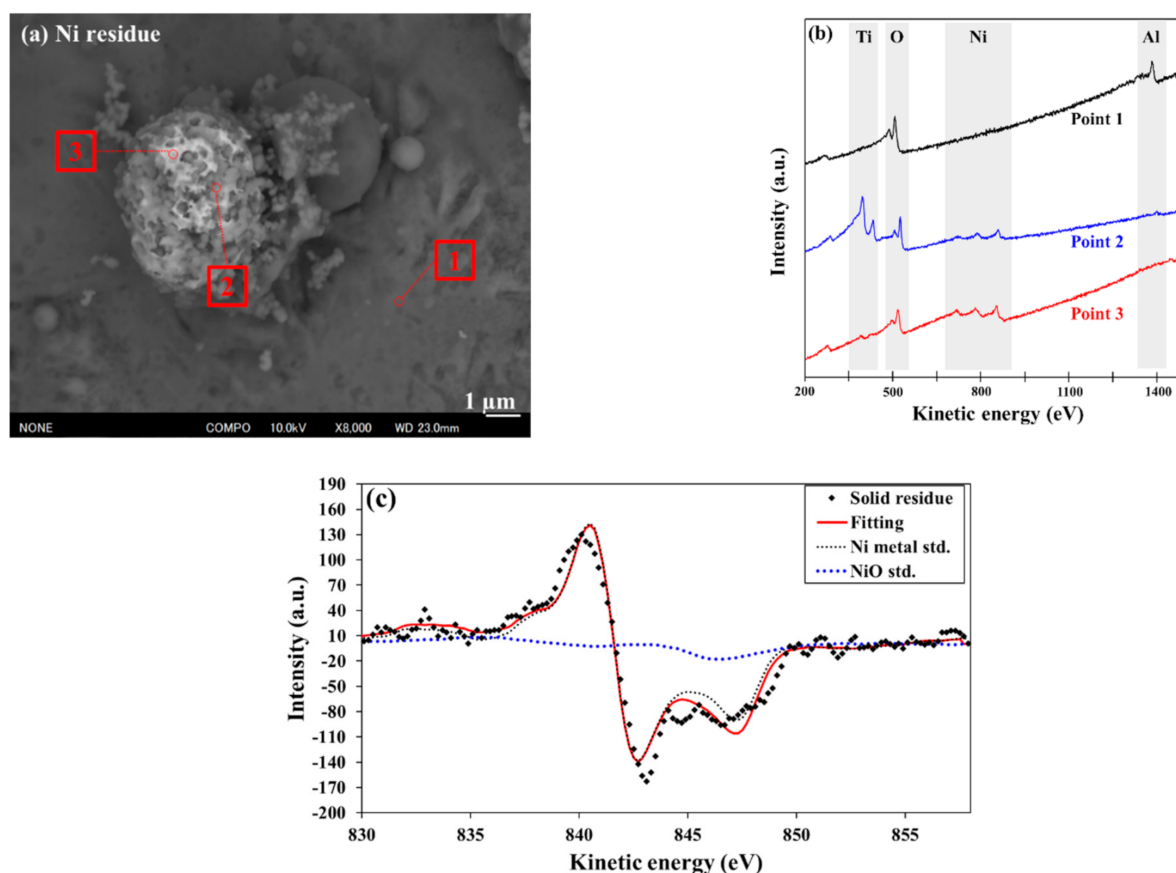
Figure 7. Auger electron spectroscopy (AES) results of the residue obtained after cementation of Ni^{2+} from chloride solution using TiO$_2$/Al: (**a**) photomicrograph, (**b**) wide scan energy spectrum of each points, and (**c**) the narrow scan energy spectrum of the Ni peak with fitting spectra of Ni and NiO.

4. Conclusions

This study investigated whether activated carbon (AC) could be replaced with other additives such as TiO$_2$ and SiO$_2$ for the enhanced cementation of Co^{2+} and Ni^{2+} using aluminum (Al) in sulfate and chloride solutions. In summary, the Co^{2+} and Ni^{2+} recovery efficiencies using Al in sulfate and chloride solutions were almost 0% because of the presence of an Al oxide layer on an Al surface. The adsorption of Co^{2+} and Ni^{2+} occurred when using only AC, while it did not occur when using only TiO$_2$ and SiO$_2$. When using an AC/Al-mixture or TiO$_2$/Al-mixture, the Co^{2+} and Ni^{2+} recovery efficiencies from sulfate and chloride solutions were enhanced compared to using Al, AC, TiO$_2$, and SiO$_2$/Al-mixture. From the results of AES analysis, Co and Ni were mostly deposited as zero-valent forms on TiO$_2$ attached to Al surface. This work establishes that using a conductor (AC) or a semiconductor (TiO$_2$) could enhance the recovery of Co^{2+} and Ni^{2+} by Al-based cementation even under mild conditions (e.g., low temperature, 25 °C; mild pH conditions, pH 4–5; no Cl$^-$ or a low concentration). Moreover, it is expected that other conductive materials could also be used for the removal and/or recovery of metal ions using Al.

using the GWB Professional Ver. 12.0.3 software), Figure S2: The activity–pH diagram for 1 mM Ni^{2+} species with 0.1 M SO_4^{2-} at 25 °C (created using the GWB Professional Ver. 12.0.3 software), Figure S3: The activity–pH diagram for 1 mM Co^{2+} species with 0.1 M Cl^- at 25 °C (created using the GWB Professional Ver. 12.0.3 software), Figure S4: The activity–pH diagram for 1 mM Ni^{2+} species with 0.1 M Cl^- at 25 °C (created using the GWB Professional Ver. 12.0.3 software).

References

1. Nelson, A.; Wang, W.; Demopoulos, G.P.; Houlachi, G. Removal of cobalt from zinc electrolyte by cementation: A critical review. *Miner. Process. Extr. Metall. Rev.* **2000**, *20*, 325–356. [CrossRef]
2. Demirkran, N.; Künkül, A. Recovering of copper with metallic aluminum. *Trans. Nonferrous Met. Soc. China* **2011**, *21*, 2778–2782. [CrossRef]
3. Silwamba, M.; Ito, M.; Hiroyoshi, N.; Tabelin, C.B. Recovery of Lead and Zinc from Zinc Plant Leach Residues by Concurrent Dissolution-Cementation. *Metals* **2020**, *10*, 531. [CrossRef]
4. Choi, S.; Yoo, K.; Alorro, R.D.; Tabelin, C.B. Cementation of Co ion in leach solution using Zn powder followed by magnetic separation of cementation-precipitate for recovery of unreacted Zn powder. *Miner. Eng.* **2020**, *145*. [CrossRef]
5. Farahmand, F.; Moradkhani, D.; Sadegh Safarzadeh, M.; Rashchi, F. Optimization and kinetics of the cementation of lead with aluminum powder. *Hydrometallurgy* **2009**, *98*, 81–85. [CrossRef]
6. Abdel-Aziz, M.H.; El-Ashtoukhy, E.S.Z.; Bassyouni, M. Recovery of Copper from Effluents by Cementation on Aluminum in a Multirotating Cylinder-Agitated Vessel. *Metall. Mater. Trans. B Process Metall. Mater. Process. Sci.* **2016**, *47*, 657–665. [CrossRef]
7. Abdollahi, P.; Yoozbashizadeh, H.; Moradkhani, D.; Behnian, D. A Study on Cementation Process of Lead from Brine Leaching Solution by Aluminum Powder. *OALib* **2015**, *2*, 1–6. [CrossRef]
8. Boisvert, L.; Turgeon, K.; Boulanger, J.; Bazin, C.; Houlachi, G. Recovery of Cobalt from the Residues of an Industrial Zinc Refinery. *Metals* **2020**, *10*, 1553. [CrossRef]
9. Li, W.; Cochell, T.; Manthiram, A. Activation of aluminum as an effective reducing agent by pitting corrosion for wet-chemical synthesis. *Sci. Rep.* **2013**, *3*, 1–7. [CrossRef]
10. Park, I.; Tabelin, C.B.; Seno, K.; Jeon, S.; Ito, M.; Hiroyoshi, N. Simultaneous suppression of acid mine drainage formation and arsenic release by Carrier-microencapsulation using aluminum-catecholate complexes. *Chemosphere* **2018**, *205*, 414–425. [CrossRef]
11. Silwamba, M.; Ito, M.; Hiroyoshi, N.; Tabelin, C.B.; Fukushima, T.; Park, I.; Jeon, S.; Igarashi, T.; Sato, T.; Nyambe, I.; et al. Detoxification of lead-bearing zinc plant leach residues from Kabwe, Zambia by coupled extraction-cementation method. *J. Environ. Chem. Eng.* **2020**, *8*, 104197. [CrossRef]
12. Annamalai, V.; Murr, L.E. Effects of the source of chloride ion and surface corrosion patterns on the kinetics of the copper-aluminum cementation system. *Hydrometallurgy* **1978**, *3*, 249–263. [CrossRef]
13. Artamonov, V.V.; Moroz, D.R.; Bykov, A.O.; Artamonov, V.P. Experimental studies of cementation of tin in a dispersed form. *Russ. J. Non-Ferrous Met.* **2013**, *54*, 128–131. [CrossRef]
14. Ekmekyapar, A.; Tanaydin, M.; Demirkiran, N. Investigation of copper cementation kinetics by rotating aluminum disc from the leach solutions containing copperions. *Physicochem. Probl. Miner. Process.* **2012**, *48*, 355–367. [CrossRef]
15. Djokić, S.S. Cementation of Copper on Aluminum in Alkaline Solutions. *J. Electrochem. Soc.* **1996**, *143*, 1300–1305. [CrossRef]
16. Jeon, S.; Tabelin, C.B.; Park, I.; Nagata, Y.; Ito, M.; Hiroyoshi, N. Ammonium thiosulfate extraction of gold from printed circuit boards (PCBs) of end-of-life mobile phones and its recovery from pregnant leach solution by cementation. *Hydrometallurgy* **2020**, *191*, 105214. [CrossRef]
17. Jeon, S.; Tabelin, C.B.; Takahashi, H.; Park, I.; Ito, M.; Hiroyoshi, N. Enhanced cementation of gold via galvanic interactions using activated carbon and zero-valent aluminum: A novel approach to recover gold ions from ammonium thiosulfate medium. *Hydrometallurgy* **2020**, *191*, 105165. [CrossRef]
18. Sulyman, M.; Namiesnik, J.; Gierak, A. Low-cost adsorbents derived from agricultural by-products/wastes for enhancing contaminant uptakes from wastewater: A review. *Polish J. Environ. Stud.* **2017**, *26*, 479–510. [CrossRef]
19. Negem, M.; Nady, H.; El-Rabiei, M.M. Nanocrystalline nickel–cobalt electrocatalysts to generate hydrogen using alkaline solutions as storage fuel for the renewable energy. *Int. J. Hydrog. Energy* **2019**, *44*, 11411–11420. [CrossRef]

20. Zhang, R.; Xia, B.; Li, B.; Lai, Y.; Zheng, W.; Wang, H.; Wang, W.; Wang, M. Study on the characteristics of a high capacity nickel manganese cobalt oxide (NMC) lithium-ion battery-an experimental investigation. *Energies* **2018**, *11*, 2275. [CrossRef]

21. Lee, B.-R.; Noh, H.-J.; Myung, S.-T.; Amine, K.; Sun, Y.-K. High-Voltage Performance of Li[Ni[sub 0.55]Co[sub 0.15]Mn[sub 0.30]]O[sub 2] Positive Electrode Material for Rechargeable Li-Ion Batteries. *J. Electrochem. Soc.* **2011**, *158*, A180. [CrossRef]

22. Liu, S.; Xiong, L.; He, C. Long cycle life lithium ion battery with lithium nickel cobalt manganese oxide (NCM) cathode. *J. Power Sources* **2014**, *261*, 285–291. [CrossRef]

23. IEA. *Global EV Outlook 2020*; OECD: Paris, France, 2020; ISBN 9789264616226.

24. Zeng, X.; Li, J.; Singh, N. Recycling of spent lithium-ion battery: A critical review. *Crit. Rev. Environ. Sci. Technol.* **2014**, *44*, 1129–1165. [CrossRef]

25. Hext, P.M.; Tomenson, J.A.; Thompson, P. Titanium dioxide: Inhalation toxicology and epidemiology. *Ann. Occup. Hyg.* **2005**, *49*, 461–472. [CrossRef]

26. Nesbitt, H.W.; Bancroft, G.M.; Davidson, R.; McIntyre, N.S.; Pratt, A.R. Minimum XPS core-level line widths of insulators, including silicate minerals. *Am. Mineral.* **2004**, *89*, 878–882. [CrossRef]

27. Chen, H.J.; Lee, C. Effects of the Type of Chelating Agent and Deposit Morphology on the Kinetics of the Copper-Aluminum Cementation System. *Langmuir* **1994**, *10*, 3880–3886. [CrossRef]

28. Gao, X.; Wu, L.; Xu, Q.; Tian, W.; Li, Z.; Kobayashi, N. Adsorption kinetics and mechanisms of copper ions on activated carbons derived from pinewood sawdust by fast H3PO4 activation. *Environ. Sci. Pollut. Res.* **2018**, *25*, 7907–7915. [CrossRef]

29. Karnib, M.; Kabbani, A.; Holail, H.; Olama, Z. Heavy metals removal using activated carbon, silica and silica activated carbon composite. *Energy Procedia* **2014**, *50*, 113–120. [CrossRef]

30. Dil, E.A.; Ghaedi, M.; Ghaedi, A.M.; Asfaram, A.; Goudarzi, A.; Hajati, S.; Soylak, M.; Agarwal, S.; Gupta, V.K. Modeling of quaternary dyes adsorption onto ZnO-NR-AC artificial neural network: Analysis by derivative spectrophotometry. *J. Ind. Eng. Chem.* **2016**, *34*, 186–197. [CrossRef]

31. Burakov, A.E.; Galunin, E.V.; Burakova, I.V.; Kucherova, A.E.; Agarwal, S.; Tkachev, A.G.; Gupta, V.K. Adsorption of heavy metals on conventional and nanostructured materials for wastewater treatment purposes: A review. *Ecotoxicol. Environ. Saf.* **2018**, *148*, 702–712. [CrossRef]

32. Park, I.; Tabelin, C.B.; Seno, K.; Jeon, S.; Inano, H.; Ito, M.; Hiroyoshi, N. Carrier-microencapsulation of arsenopyrite using Al-catecholate complex: Nature of oxidation products, effects on anodic and cathodic reactions, and coating stability under simulated weathering conditions. *Heliyon* **2020**, *6*, e03189. [CrossRef] [PubMed]

33. Murr, L.E.; Annamalai, V. An Electron Microscopic Study of Nucleation and Growth in Electrochemical Displacement Reactions: A Comparison of the Cu/Fe and Cu/Al Cementation Systems. *Metall. Trans. B* **1978**, *9*, 515–525. [CrossRef]

34. Murr, L.E.; Annamalai, V. Characterization of copper nucleation and growth from aqueous solution on aluminum: A transmission electron microscopy study of copper cementation. *Thin Solid Films* **1978**, *54*, 189–195. [CrossRef]

35. Reboul, M.C.; Warner, T.J.; Mayer, H.; Barouk, B. A Ten Step Mechanism for the Pitting Corrosion of Aluminium Alloys. *Corros. Rev.* **1997**, *15*, 471–496. [CrossRef]

36. Andersson, M.; Kiselev, A.; Österlund, L.; Palmqvist, A.E.C. Microemulsion-mediated room-temperature synthesis of high-surface-area rutile and its photocatalytic performance. *J. Phys. Chem. C* **2007**, *111*, 6789–6797. [CrossRef]

37. Inada, M.; Mizue, K.; Enomoto, N.; Hojo, J. Synthesis of rutile TiO2 with high specific surface area by self-hydrolysis of TiOCl2 in the presence of SDS. *J. Ceram. Soc. Jpn.* **2009**, *117*, 819–822. [CrossRef]

38. Scherer, J. Auger Electron Spectroscopy (AES): A Versatile Microanalysis Technique in the Analyst's Toolbox. *Microsc. Microanal.* **2020**, *26*, 1564–1565. [CrossRef]